ORIGINAL RESEARCH

Redox and Activation of Protein Kinase A Dysregulates Calcium Homeostasis in Pulmonary Vein Cardiomyocytes of Chronic Kidney Disease

Shih-Yu Huang, MD; Yao-Chang Chen, PhD; Yu-Hsun Kao, PhD; Ming-Hsiung Hsieh, MD; Yung-Kuo Lin, MD, PhD; Shih-Ann Chen, MD; Yi-Jen Chen, MD, PhD

***Background*—**Chronic kidney disease (CKD) increases the occurrence of atrial fibrillation and pulmonary vein (PV) arrhythmogenesis. Calcium dysregulation and reactive oxygen species (ROS) enhance PV arrhythmogenic activity. The purposes of this study were to investigate whether CKD modulates PV electrical activity through dysregulation of calcium homeostasis and ROS.

***Methods and Results*—**Biochemical and electrocardiographic studies were conducted in rabbits with and without CKD (induced by 150 mg/kg per day neomycin sulfate and 500 mg/kg per day cefazolin). Confocal microscopy with fluorescence and a whole-cell patch clamp were applied to study calcium homeostasis and electrical activities in control and CKD isolated single PV cardiomyocytes with or without treatment with H89 (1 μmol/L, a protein kinase A inhibitor) and MPG (N-[2-mercaptopropionyl] glycine; 100 μmol/L, a ROS scavenger). The ROS in mitochondria and cytosol were evaluated via intracellular dye fluorescence and lipid peroxidation. CKD rabbits had excessive atrial premature captures over those of control rabbits. Compared with the control, CKD PV cardiomyocytes had a faster beating rate and larger calcium transient amplitudes, sarcoplasmic reticulum calcium contents, sodium/calcium exchanger currents, and late sodium currents but smaller L-type calcium current densities. CKD PV cardiomyocytes had a higher frequency and longer duration of calcium sparks and more ROS in the mitochondria and cytosol than did controls. Moreover, H89 suppressed all calcium sparks in CKD PV cardiomyocytes, and H89- and MPG-treated CKD PV cardiomyocytes had similar calcium transients compared with control PV cardiomyocytes.

***Conclusions*—**CKD increases PV arrhythmogenesis with enhanced calcium-handling abnormalities through activation of protein kinase A and ROS. **(*J Am Heart Assoc*. 2017;6:e005701. DOI: 10.1161/JAHA.117.005701.)**

Key Words: atrial fibrillation • calcium regulation • chronic kidney disease • pulmonary vein • reactive oxygen species

Atrial fibrillation (AF), the most common clinical arrhythmia, causes significant cardiovascular morbidity and mortality due to heart failure and stroke.[1,2] AF is produced by the trigger activity from ectopic foci in the pulmonary vein (PV).[3,4] Patients with AF have abnormal calcium regulation with increasing calcium sparks and calcium leak.[5–7] In addition, calcium spark and calcium leak play critical roles in the arrhythmogenesis of PV cardiomyocytes.[7,8] Atrial PKA (protein kinase A) or CaMKII (calcium/calmodulin-dependent protein kinase II) are enhanced with increasing phosphorylation of the type 2 ryanodine receptor (RyR2), leading to great sarcoplasmic reticulum (SR) calcium leak and calcium spark.[7,9]

Chronic kidney disease (CKD) with increased albuminuria is associated with a higher prevalence of AF.[10–12] Renal failure can induce oxidative stress, inflammation, hypertension, and activation of angiotensin II and the sympathetic nervous system of the heart, which all contribute to AF genesis.[13,14]

From the Graduate Institute of Clinical Medicine (S.-Y.H., Y.-H.K., Y.-J.C.) and Division of Cardiology, Department of Internal Medicine, School of Medicine (M.-H.H., Y.-K.L.), College of Medicine, Taipei Medical University, Taipei, Taiwan; Division of Cardiology, Department of Internal Medicine, Cathay General Hospital, Taipei, Taiwan (S.-Y.H.); Department of Biomedical Engineering, National Defense Medical Center, Taipei, Taiwan (Y.-C.C.); Department of Medical Education and Research (Y.-H.K.) and Division of Cardiovascular Medicine, Department of Internal Medicine (M.-H.H., Y.-K.L., Y.-J.C.), Wan Fang Hospital, Taipei Medical University, Taipei, Taiwan; School of Medicine, National Yang-Ming University, Taipei, Taiwan (S.-A.C.); Division of Cardiology and Cardiovascular Research Center, Veterans General Hospital-Taipei, Taipei, Taiwan (S.-A.C.).

Correspondence to: Yi-Jen Chen, MD, PhD, Division of Cardiovascular Medicine, Department of Internal Medicine, Wan Fang Hospital, Taipei Medical University, 111 Hsin-Lung Road, Sec. 3, Taipei 116, Taiwan. E-mail: a9900112@ms15.hinet.net

Received January 25, 2017; accepted June 1, 2017.

Clinical Perspective

What Is New?

- Chronic kidney disease (CKD) increases pulmonary vein arrhythmogenesis with abnormal calcium homeostasis.
- Reactive oxygen species and modulation of calcium-regulation protein kinase are key mechanisms underlying the genesis of calcium dysregulation and arrhythmogenesis in CKD pulmonary vein cardiomyocytes.

What Are the Clinical Implications?

- Our findings support that enhanced redox signaling and protein kinase A activity have a critical impact on calcium homeostasis of pulmonary vein arrhythmogenesis contributing to atrial arrhythmia in CKD.
- Abnormal calcium handling in CKD pulmonary vein cardiomyocytes is inhibited by the antioxidant and protein kinase A inhibitor, which may lead to an innovative treatment strategy in CKD patients with atrial fibrillation.

A previous experiment demonstrated that an antioxidant agent could suppress pacing-induced AF in fibrotic cardiomyocytes in a nephrectomy-induced renal dysfunction animal model.[15] Our previous study showed that increased protein expressions of PKA, RyR2 pS2808 (phosphorylated RyR2 at serine 2808), and PLB pSer16 (phosphorylated phospholamban [PLB] at serine 16) in CKD may enhance PV arrhythmogenesis, which contributes to a high risk of AF.[16] Increased oxidative stress and PKA are found in the renal cortex of CKD rats, resulting in dysregulated cellular calcium homeostasis.[17,18] High mitochondrial reactive oxygen species (ROS) stimulate kinase activity, leading to calcium-handling abnormalities.[18–20] In addition, ROS may enhance the sodium/calcium exchanger (NCX) and increase the frequency of calcium sparks by activating PKA phosphorylation.[18,21,22] Nevertheless, knowledge of interactions of calcium homeostasis and ROS in CKD and their role in CKD-induced PV arrhythmogenesis is limited. The purposes of this study were to investigate whether CKD modulates PV electrical activity through dysregulation of calcium homeostasis and to assess the potential mechanisms of ROS-related CKD PV arrhythmogenesis.

Methods

CKD Animal Preparation

All experimental procedures were completed in accordance with guidelines from the institutional animal care and use committee. CKD and control rabbits (3.0–3.5 kg) received an intraperitoneal injection of neomycin sulfate (150 mg/kg per day) and cefazolin (500 mg/kg per day) or vehicle every other day for 4 weeks.[16] Biochemical examinations of serum and urine were performed. ECGs of the rabbits were recorded by connecting their 4 limbs to the cable leads of a digital Holter ECG recorder for 6 hours twice a week, as described previously.[16] Excessive atrial premature complexes (APCs) were defined as ≥30 APCs per hour or any episode with ≥20 APCs. Rabbits with high serum creatinine (>6.0 mg/dL), a large amount of proteinuria, and a high urine microalbumin: creatinine ratio were classified as CKD, as shown in Table.[23]

Table. Biochemical and Physiological Properties of Control and CKD Rabbits

	Control (n=15)	CKD (n=15)	*P* Value
BUN, mg/dL	17.3±0.9	107.1±20.8	0.002
Creatinine, mg/dL	0.92±0.29	7.32±0.83	<0.001
Hemoglobin, g/dL	13.7±0.35	10.6±0.33	<0.001
Hematocrit, %	43.6±1.25	35.3±1.1	<0.001
Albumin, g/dL	3.57±0.06	3.08±0.11	0.001
Sodium, mmol/L	140.6±0.8	144.4±2.2	0.15
Potassium, mmol/L	4.8±0.19	4.3±0.25	0.126
Calcium, mg/dL	13.1±0.2	9.4±0.71	<0.001
Phosphate, mg/dL	7.4±0.21	13.3±2.1	0.016
Magnesium, mg/dL	2.61±0.08	2.58±0.21	0.137
Proteinuria, mg/dL	37.3±12.1	193.3±26.7	<0.001
Microalbuminuria, mg/dL	6.33±1.25	188.2±53.8	<0.001
UACR, mg/g	27.5±4.4	714.5±135.4	<0.001
With excessive APCs, %	0	53.4	0.002
With SVT, %	0	20.0	0.224

APCs indicates atrial premature complexes; BUN, blood urea nitrogen; CKD, chronic kidney disease; SVT, supraventricular tachycardia; UACR, urine albumin:creatinine ratio.

Single PV Cardiomyocyte Isolation

As described previously, PV cardiomyocytes of control and CKD rabbits were enzymatically dissociated after rabbits were anesthetized with an intraperitoneal injection of sodium pentobarbital (100 mg/kg).[8] In brief, a midline thoracotomy was performed, and the heart and lungs were removed. PVs were perfused in a retrograde manner via polyethylene tubing cannulated through the aorta and left ventricle into the left atrium. The free end of the polyethylene tube was connected to a Langendorff perfusion column for perfusion with oxygenated normal Tyrode's solution (containing [in mmol/L] NaCl 137, KCl 5.4, $CaCl_2$ 1.8, $MgCl_2$ 0.5, HEPES 10, and glucose 11; with the pH adjusted to 7.4 by titration with 1 N NaOH). The perfusate was replaced with oxygenated Ca^{2+}-free Tyrode's solution containing 300 U/mL collagenase (type I)

and 0.25 U/mL protease (type XIV) for 8 to 12 minutes. Isolated single CKD PV cardiomyocytes were pretreated with or without H89 (1 μmol/L, an inhibitor of PKA), KN93 (1 μmol/L, an inhibitor of CaMKII), KN92 (1 μmol/L, an inactive analog of KN93), ranolazine (10 μmol/L, an inhibitor of late sodium current [$I_{Na\text{-}Late}$]), and MPG (N-[2-mercaptopropionyl]glycine; 100 μmol/L, a ROS scavenger) for 1 minute before recording.

Measurements of Intracellular Calcium, SR Calcium Contents, and Calcium Spark Imaging

PV cardiomyocytes from both control and CKD rabbits were loaded with fluorescent Ca^{2+} (10 μmol/L, fluo-3/AM) for 30 minutes at room temperature, as described previously.[8,24] Fluo-3 fluorescence was excited by a 488-nm line of an argon ion laser. The emission was recorded at >515 nm. Cells were repetitively scanned at 2-ms intervals. Fluorescence imaging was performed with a laser scanning confocal microscope (Zeiss LSM 510, Carl Zeiss) and an inverted microscope (Axiovert 100, Carl Zeiss). Fluorescent signals were corrected for variations in dye concentrations by normalizing the fluorescence (represented by F) against baseline fluorescence (F_0) to obtain reliable information about transient intracellular Ca^{2+} (Ca^{2+}i) changes from baseline values, as $(F-F_0)/F_0$, and to exclude variations in the fluorescence intensity by different volumes of injected dye. The Ca^{2+}i transient, peak systolic Ca^{2+}i, and diastolic Ca^{2+}i were measured during a 2-Hz field stimulation with 10-ms, twice-threshold-strength, square-wave pulses. After achieving steady-state Ca^{2+} transients with repeated pulses from −40 to 0 mV (1 Hz for 5 seconds), the total amount of charge crossing the membrane SR Ca^{2+} content (represented as Ccaff in the equation) was estimated by integrating the NCX current after rapid application of 20 mmol/L caffeine during rest with the membrane potential clamped at −40 mV to cause SR Ca^{2+} release. The NCX current was measured by whole-cell patch clamp experiments. The total SR Ca^{2+} content (expressed as mmol/L of cytosol) was determined using the equation SR Ca^{2+} content= $[(1+0.12)\ (Ccaff/F\times 1000)]/(Cm\times 8.31\times 6.44)$, where Cm is the membrane capacitance, F is Faraday's number, and the cell surface:volume ratio was 6.44 pF/pL.

Calcium sparks were detected using the line scan mode along a line parallel to the longitudinal axis of single PV cardiomyocytes while avoiding nuclei. Each line was composed of 512 pixels. Calcium sparks were detected as an increase in the signal mass (>1.3 F/F_0) of a 5-μm section through the center of a calcium spark, with no detectable increase in an adjacent 5-μm section. The amplitude, duration, diameter, time to the peak, and half-life of each calcium spark were determined from an exponential fit of the decay phase of the transient calcium spark. The calcium spark frequency was determined for each cell and normalized to the scanned cell length before and after drug administration. Images were analyzed using both ImageJ (National Institutes of Health) and custom-made routines based on IDL (ITT Visual information Solutions).

Patch Clamp Experiments

A whole-cell patch clamp was used on PV cardiomyocytes with an Axopatch 1D amplifier (Axon Instruments) at 35±1°C. The micropipette resistance was 3 to 5 MΩ. A small hyperpolarizing step from a holding potential of −50 mV to a test potential of −55 mV for 80 ms was delivered at the beginning of each experiment. The micropipette resistance was 3 to 5 MΩ. The area under the capacitative currents curve was divided by the applied voltage step to obtain the total cell capacitance. Normally, 60% to 80% series resistance was electronically compensated for. Action potential recordings were made in the current-clamp mode, and ionic currents were recorded in the voltage-clamp mode.[24–26] Ionic currents and action potentials were recorded in an approximately similar period (3–5 minutes) after rupture or perforation to avoid decay of ion channel activity over time. Micropipettes were filled with a solution containing (in mmol/L) KCl 20, K aspartate 110, $MgCl_2$ 1, MgATP 5, HEPES 10, EGTA 0.5, NaGTP 0.1, and Na_2 phosphocreatine 5, titrated to pH 7.2 with KOH for experiments on the action potential; with a solution containing (in mmol/L) NaCl 20, CsCl 110, $MgCl_2$ 0.4, $CaCl_2$ 1.75, tetraethylammonium chloride 20, BAPTA 5, glucose 5, MgATP 5, and HEPES 10, titrated to pH 7.25 with CsOH for experiments on the NCX current; with a solution containing (in mmol/L) CsCl 130, $MgCl_2$ 1, MgATP 5, HEPES 10, EGTA 10, NaGTP 0.1, and Na_2 phosphocreatine 5, titrated to pH 7.2 with CsOH for experiments on the L-type calcium current; and with a solution containing (in mmol/L) CsCl 130, Na_2ATP 4, $MgCl_2$ 1, EGTA 10, and HEPES 5 at pH 7.3 with NaOH for $I_{Na\text{-}Late}$.

The NCX current was elicited by test pulses of between −100 and +100 mV from a holding potential of −40 mV for 300 ms at a frequency of 0.1 Hz. Amplitudes of the NCX current were measured as 10-mmol/L nickel-sensitive currents. The external solution consisted of (in mmol/L) NaCl 140, $CaCl_2$ 2, $MgCl_2$ 1, HEPES 5, and glucose 10 at pH 7.4 and contained strophanthidin (10 μmol/L), nitrendipine (10 μmol/L), and niflumic acid (100 μmol/L).

The L-type calcium current was measured as an inward current during depolarization from a holding potential of −50 mV to test potentials ranging from −40 to +60 mV in 10-mV steps for 300 ms at a frequency of 0.1 Hz by means of a perforated patch clamp with amphotericin B. NaCl and KCl in the external solution were respectively replaced with tetraethylammonium chloride and CsCl. To avoid "run-down" effects, the L-type calcium current was measured at 5 to

15 minutes after rupturing the membrane patch in each PV cardiomyocyte.

The $I_{Na\text{-}Late}$ was recorded at room temperature with an external solution containing (in mmol/L) NaCl 130, CsCl 5, $MgCl_2$ 1, $CaCl_2$ 1, HEPES 10, and glucose 10 at pH 7.4 with NaOH by a step/ramp protocol (−100 mV stepped to +20 mV for 100 ms, then ramped back to −100 mV over 100 ms). The $I_{Na\text{-}late}$ was measured as the tetrodotoxin (30 μmol/L)–sensitive portions of the current traces obtained when the voltage was ramped back to −100 mV.

Western Blot Analysis

Control and CKD PV cardiomyocytes were centrifuged and washed with cold PBS and lysed on ice for 30 minutes in RIPA buffer containing 50 mmol/L Tris, pH 7.4, 150 mmol/L NaCl, 1% NP40, 0.5% sodium deoxycholate, 0.1% sodium dodecyl-sulfate, and protease inhibitor cocktails. The protein concentrations were determined with a Bio-Rad protein assay reagent. Proteins were separated in 4% to 12% SDS-PAGE under reducing conditions and electrophoretically transferred into an equilibrated polyvinylidene difluoride membrane. All blots were probed with primary antibodies against PKA, RyR2, PLB, PLB pSer16, RyR2 pS2808, RyR2 pS2814, and PLB pThr17 (phosphorylated PLB at threonine 17), GAPDH, and all secondary antibodies conjugated with horseradish peroxidase. All bound antibodies were detected with an enhanced chemiluminescence detection system and analyzed with AlphaEaseFC software. All targeted bands were normalized to GAPDH to confirm equal protein loading.

SR Ca^{2+}-ATPase Activity

The ATPase activity of the cardiac SR Ca^{2+} pump was measured using an enzyme-coupled assay.[27] SR vesicles were prepared from PV cardiomyocytes, as described by Münch et al.[28] SR protein (25 μg) was incubated in 250 μL buffer containing 21 mmol/L MOPS, 100 mmol/L KCl, 3 mmol/L $MgCl_2$, 0.06 mmol/L EGTA, 4.9 mmol/L NaN_3, 1 mmol/L glycerophosphate, 1 mmol/L phosphoenopyruvate, 0.1 mmol/L NADH, 8.4 U pyruvate kinase, and 12 U lactate dehydrogenase. The reactions received 1 mmol/L of ATP at 30°C (basal activity). SR Ca^{2+}-ATPase (SERCA2a) activity was measured as the change in absorption at 340 nm divided by the extinction coefficient of NADH. The consumption of NADH is considered to be equivalent to the hydrolysis of ATP by SERCA2a at 1 μmol/L $CaCl_2$.

Measurement of Intracellular ROS

Experiments were also performed using a laser scanning confocal microscope (Zeiss LSM 510, Carl Zeiss) and an inverted microscope (Axiovert 100, Carl Zeiss) with a 60×1.4 numerical aperture oil immersion objective, as described previously.[19] PV cardiomyocytes were maintained in oxygenated normal Tyrode's solution (containing [in mmol/L] NaCl 137, KCl 5.4, $CaCl_2$ 1.8, $MgCl_2$ 0.5, HEPES 10, and glucose 11; with the pH adjusted to 7.4 by titration with 1 N NaOH) supplemented with the appropriate fluorescent dye of 5 μmol/L MitoSOX Red (Life Technologies). MitoSOX Red was excited at 488 nm, and fluorescence signals were acquired at wavelengths of >505 nm in the XY mode of the confocal system. Fluorescent images were analyzed using Image-Pro Plus 6.0 and SigmaPlot 12.3 software.

The level of malondialdehyde in rabbit plasma and PV cardiomyocytes to detect lipid peroxidation were assessed by an ELISA kit, according to the manufacturer's guidelines and a colorimetric-fluorimetric method.

Statistical Analysis

All quantitative data are expressed as the mean±SEM. Comparisons between the control and CKD rabbits or PV cardiomyocytes were analyzed by a Mann–Whitney *U* test. A Wilcoxon signed rank test was used to compare the difference before and after treatment of CKD PV cardiomyocytes. Nominal variables were compared by a χ^2 analysis or Fisher exact test if >20% of the expected cell frequencies were <5. A *P* value of <0.05 was considered statistically significant.

Results

Electrical Activity and Calcium Homeostasis in CKD and Control PV Cardiomyocytes

As shown in Table and Figure 1, CKD rabbits (n=15) had excessive APCs compared with control rabbits (n=15), and CKD PV cardiomyocytes (n=8, from 4 hearts) had a faster beating rate (2.61±0.18 versus 1.98±0.21 Hz) than control PV cardiomyocytes (n=10, from 4 hearts). Although AF was not found in either group, CKD rabbits tended to have a higher incidence of supraventricular tachycardia than control rabbits. CKD PV cardiomyocytes had larger SR calcium contents and calcium transient amplitudes (1.08±0.13 versus 0.68±0.09 mmol/L of cytosol and 2.31±0.15 versus 1.50±0.08 F/F_0, respectively) than did control PV cardiomyocytes (Figure 2A). As shown in Figure 2B, the western blot showed larger expressions of PKA, PLB pSer16, and RyR2 pS2808 in CKD PVs than in control PVs; however, there were similar expressions of PLB, PLB pThr17, RyR2, and RyR2 pS2814 in control and CKD PVs. In addition, compared with control PVs, CKD PVs had higher SERCA2a activity (relative to control, 1.48±0.12 versus 1.00±0.12 nmol ATP×mg protein^{-1}×min^{-1}; Figure 2C). As shown in Figure 3, CKD PV

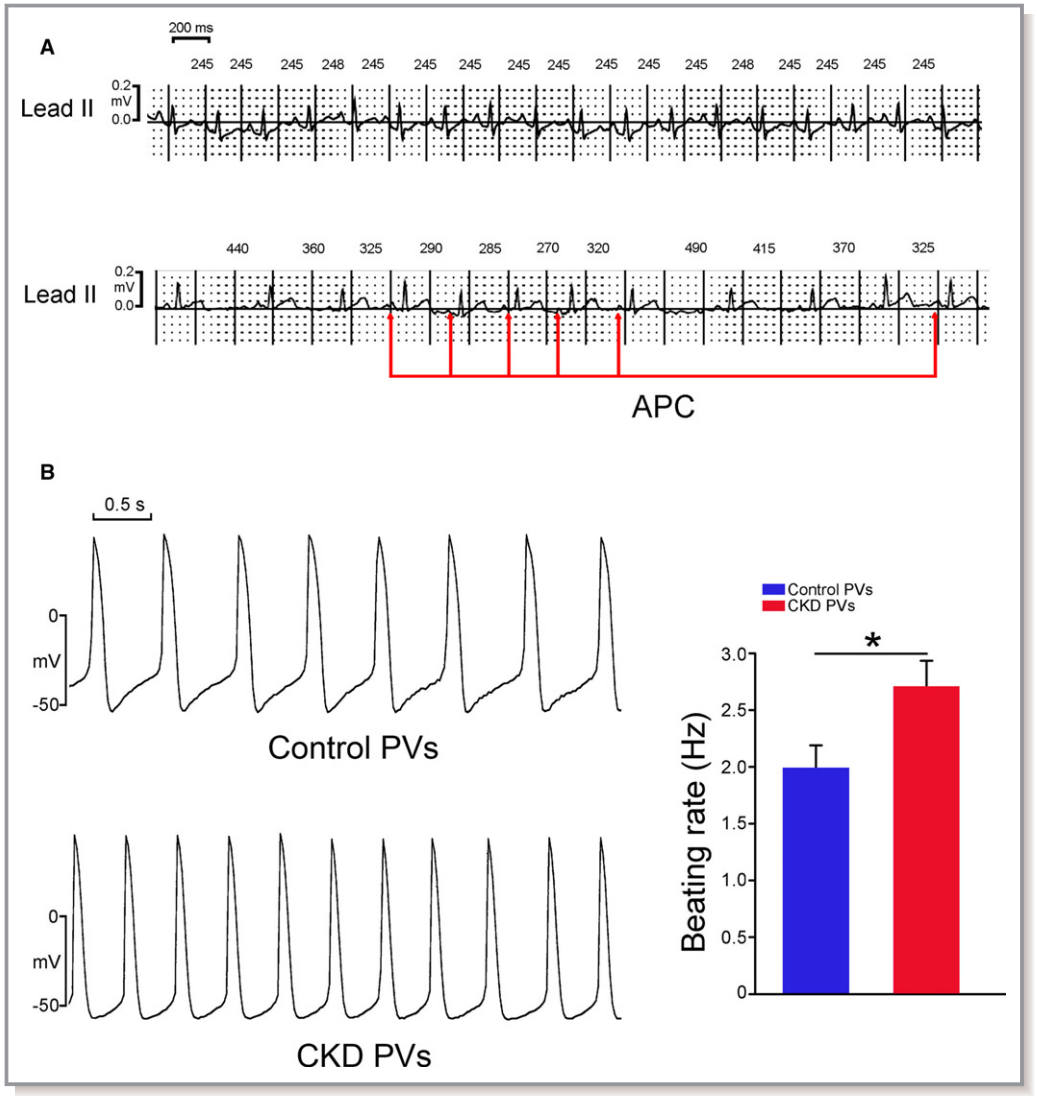

Figure 1. Electrocardiography and spontaneous beating rates of pulmonary vein (PV) cardiomyocytes in control and chronic kidney disease (CKD) rabbits. A, Control rabbits had a regular beating rate, but CKD rabbits had repeated atrial premature complexes (↑, APCs). B, An example and average data show that CKD PV cardiomyocytes (n=8, from 4 hearts) had more rapid beating rates than control PV cardiomyocytes (n=10, from 4 hearts). **P*<0.05 vs the control.

cardiomyocytes treated with H89 (1 μmol/L) and KN93 (1 μmol/L) had smaller calcium transients (1.52±0.11 versus 2.24±0.23 F/F_0 and 2.02±0.22 versus 2.28±0.17 F/F_0, respectively) than did CKD PV cardiomyocytes. H89, however, produced a greater decrease in calcium transients than did KN93 (−29.43±4.70% versus −12.32±3.54%, *P*<0.05).

As shown in Figure 4A, compared with control PV cardiomyocytes, CKD PV cardiomyocytes had a higher frequency of calcium sparks (4.96±0.73 versus 2.35±0.30 sparks/mm per second) with a longer duration (210.66±18.76 versus 137.44±11.22 ms), width (4.42±0.37 versus 3.32±0.17 ms), time to peak (92.64±11.95 versus 63.07±6.47 ms), and decay time (117.87±9.86 versus 77.74±8.05 ms). Moreover, CKD PV cardiomyocytes had a higher incidence of spontaneous calcium releases along the calcium spark than did control PV cardiomyocytes (41.39% versus 8.00%, Figure 4B). Furthermore, in CKD PV cardiomyocytes (n=6, from 4 hearts) that presented calcium sparks, H89 (1 μmol/L) completely eliminated calcium sparks. In contrast, KN93 eliminated calcium sparks in 3 (50%) of 6 CKD PV cardiomyocytes (from 4 hearts) and reduced the frequency of calcium sparks from 4.73±0.19 to 2.37±0.48 sparks/mm per second (*P*<0.05), whereas KN92 eliminated calcium sparks in 1 (20%) of 5 CKD PV cardiomyocytes (from 4 hearts) and reduced the frequency of calcium sparks from 4.71±0.93 to 3.00±0.84 sparks/mm per second (*P*>0.05).

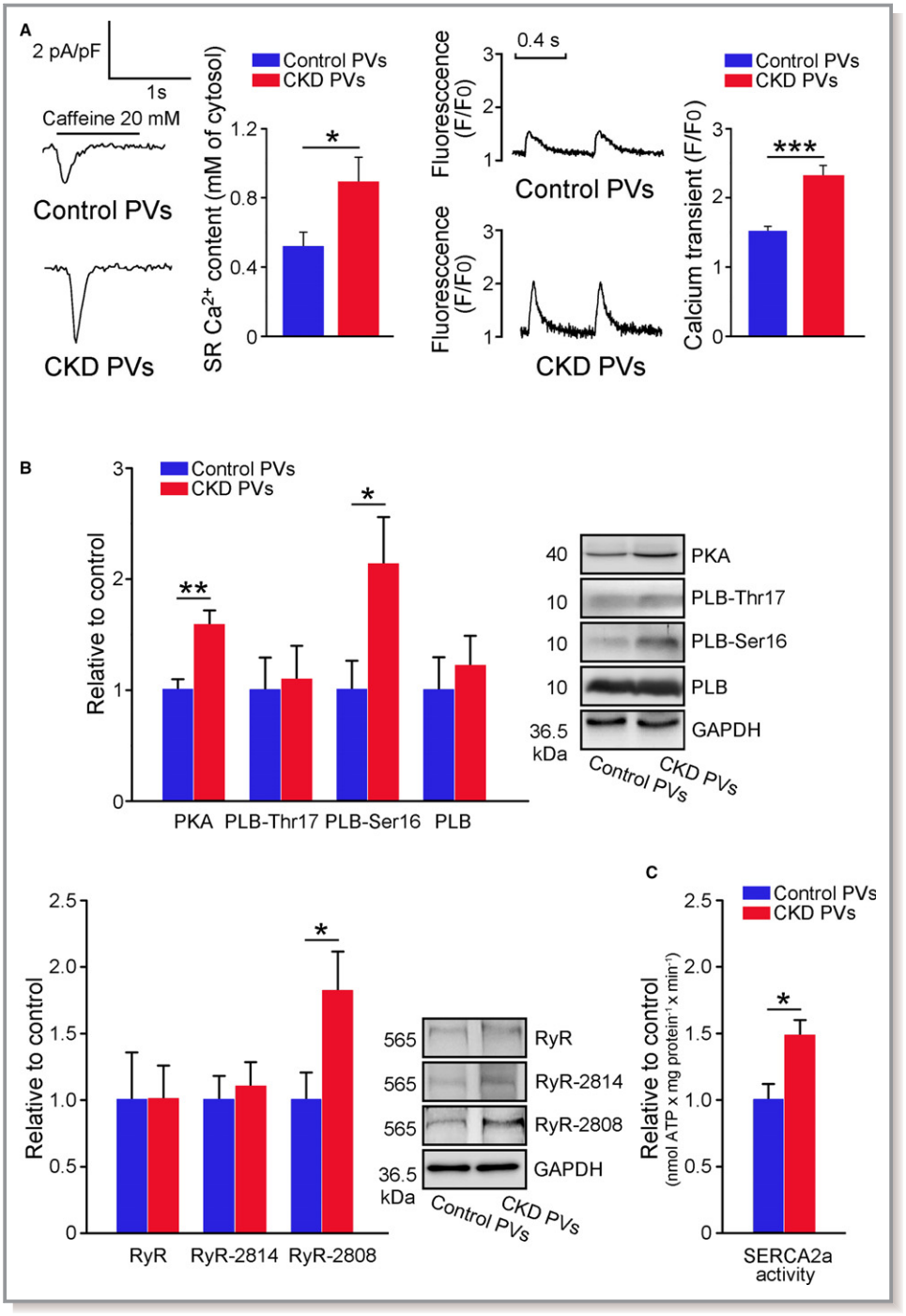

Figure 2. Intracellular calcium homeostasis, calcium regulatory protein, and sarcoplasmic reticulum (SR) Ca^{2+}-ATPase (SERCA2a) activity in control and chronic kidney disease (CKD) pulmonary vein (PV) cardiomyocytes. A, Tracings and average data of SR calcium contents (left panels) from integrating caffeine-induced sodium/calcium exchanger (NCX) currents in control (n=12, from 4 hearts) and CKD (n=10, from 4 hearts) PV cardiomyocytes. Tracings and average data of calcium transients from 2-Hz field stimulation (right panels) in control (n=14, from 5 hearts) and CKD (n=12, from 6 hearts) PV cardiomyocytes. B, Representative immunoblot and average data of PKA, phosphorylated phospholamban (PLB) at PLB pThr17 (phosphorylated PLB at threonine 17), PLB pSer16 (phosphorylated PLB at serine 16), PLB, type 2 ryanodine receptor (RyR2) channels, RyR2 pS2814 (phosphorylated RyR2 at serine 2814), RyR2 pS2808 (phosphorylated RyR2 at serine 2808), from control (from 8 hearts) and CKD PV cardiomyocytes (from 8 hearts). C, The SERCA2a activity was higher in CKD PV cardiomyocytes (from 7 hearts) than control PV cardiomyocytes (from 6 hearts). *P<0.05, **P<0.01, ***P<0.005 vs the control.

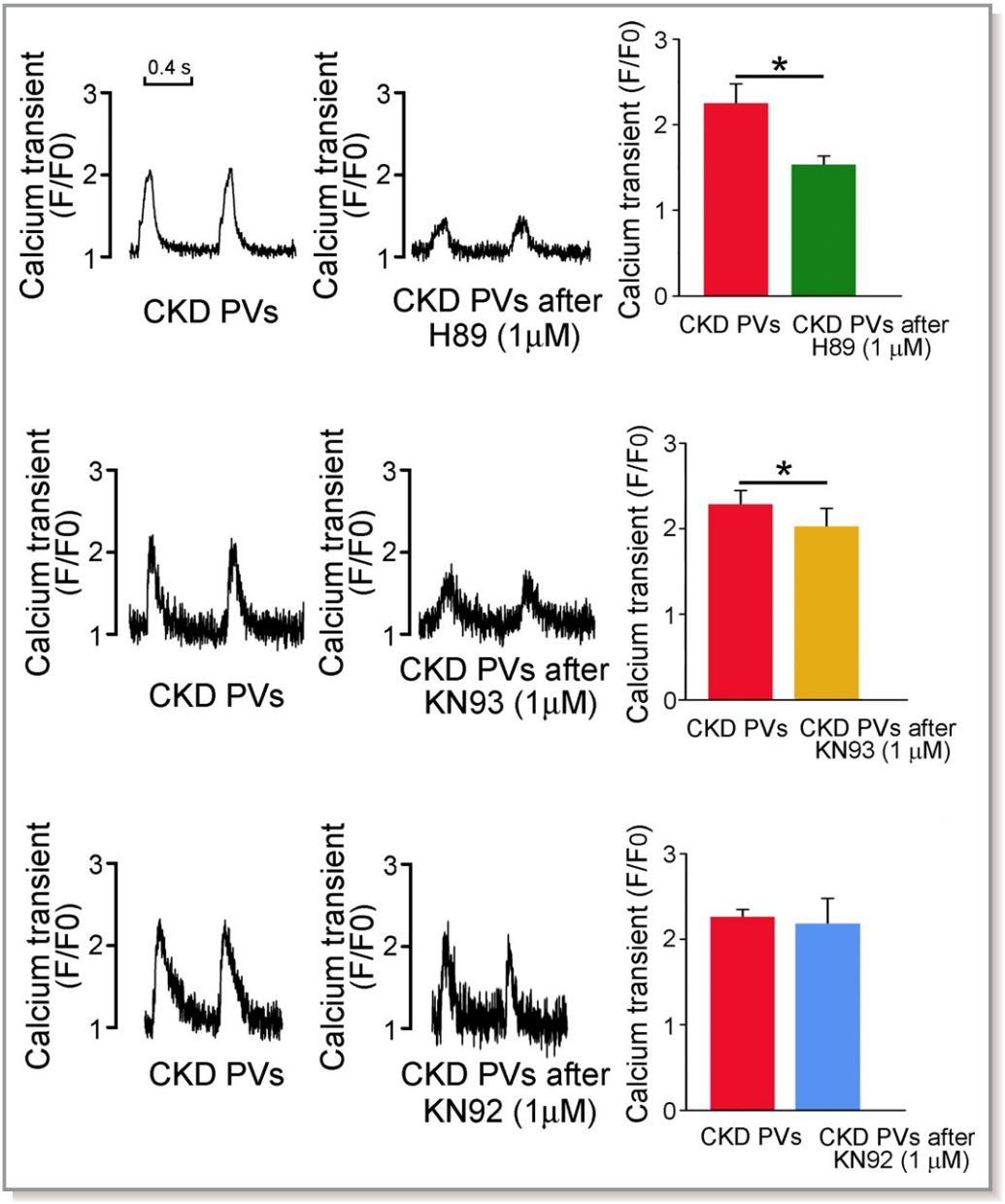

Figure 3. The effect of calcium regulation signaling in control and chronic kidney disease (CKD) pulmonary vein (PV) cardiomyocytes. Tracings and average data of calcium transients from 2-Hz field stimulation in CKD PV cardiomyocytes before and after treatment with H89 (1 μmol/L, an inhibitor of PKA; n=8, from 4 hearts), KN93 (1 μmol/L, an inhibitor of CaMKII; n=8, from 3 hearts), and KN92 (1 μmol/L, an inactive analog of KN93; n=8, from 3 hearts). **P*<0.05.

As shown in Figure 5, CKD PV cardiomyocytes had higher NCX currents and $I_{Na\text{-}Late}$ (1.15±0.12 versus 0.64±0.05 pA/pF) than did control PV cardiomyocytes; however, CKD PV cardiomyocytes had smaller L-type calcium current densities than did control PV cardiomyocytes. We studied the role of $I_{Na\text{-}Late}$ in calcium transient in PV cardiomyocytes (Figure 6) and found that *Anemonia sulcata* toxin (100 nmol/L, an enhancer of $I_{Na\text{-}Late}$) increased calcium transient in control PV cardiomyocytes (1.62±0.15 versus 2.05±0.28 F/F_0), and ranolazine (10 μmol/L) decreased calcium transient in CKD PV cardiomyocytes (2.33±0.16 versus 1.80±0.09 F/F_0).

ROS Production by CKD and Control PV Cardiomyocytes

As shown in Figure 7, CKD PV cardiomyocytes had higher ROS in mitochondria (22.64±1.91% versus 59.89±3.79%) than did control PV cardiomyocytes. CKD rabbits (n=6) had

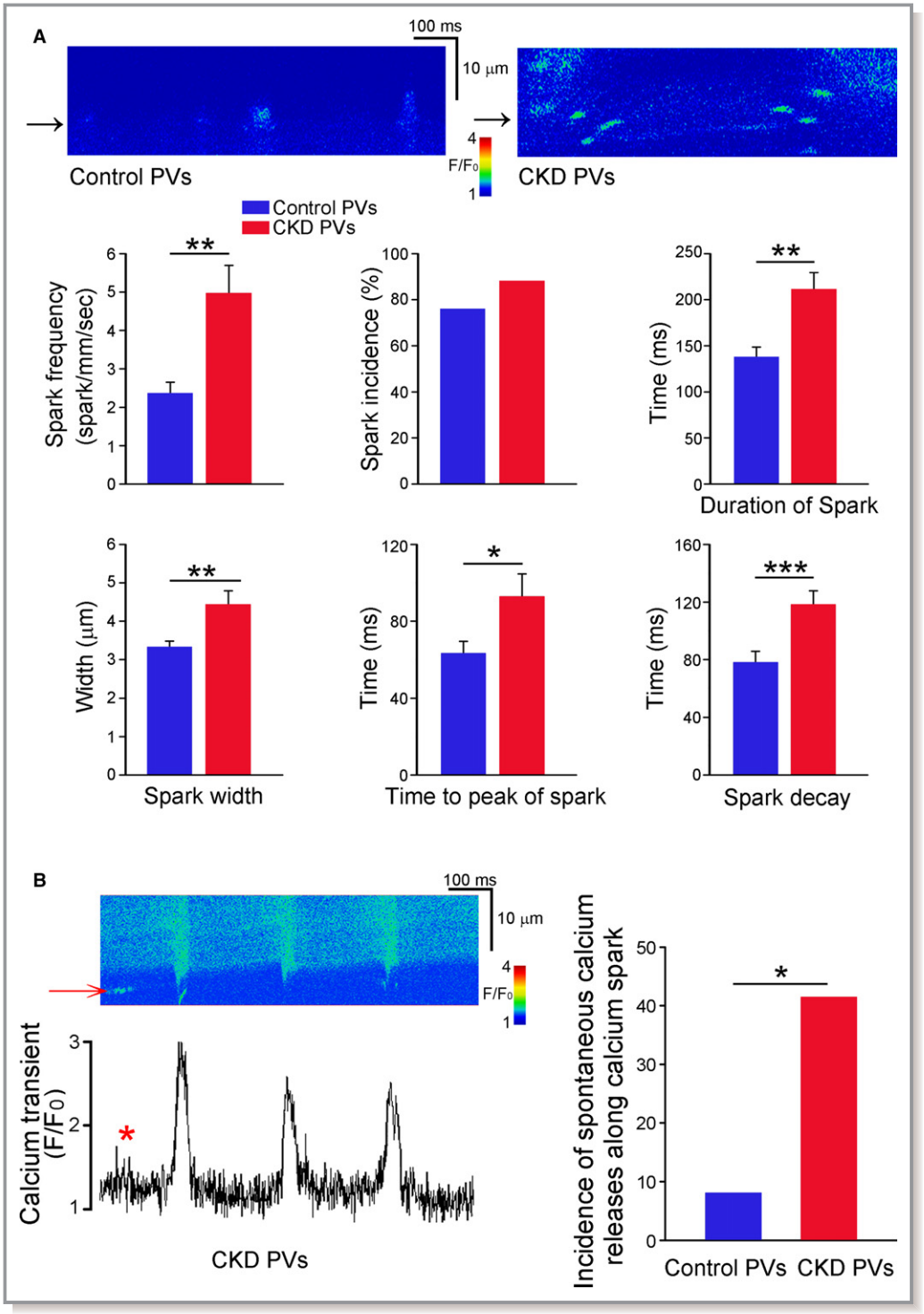

Figure 4. Calcium sparks in control and chronic kidney disease (CKD) pulmonary vein (PV) cardiomyocytes. A, Examples of line scans to detect calcium sparks in control and CKD PV cardiomyocytes. Average data of the frequency, incidence of calcium sparks, duration, width, peak time, and decay time in control (n=33, from 7 hearts) and CKD PV cardiomyocytes (n=33, from 10 hearts). B, Examples of line scans to detect spontaneous calcium releases presented along with calcium spark in CKD PV cardiomyocytes. The spontaneous calcium releases (red asterisk) that precedes ectopic activity is presented along with a calcium spark (red arrow). The incidence of spontaneous calcium releases along the calcium spark in control (n=25, from 7 hearts) and CKD PV cardiomyocytes (n=29, from 10 hearts). **P*<0.05, ***P*<0.01, ****P*<0.005 vs the control.

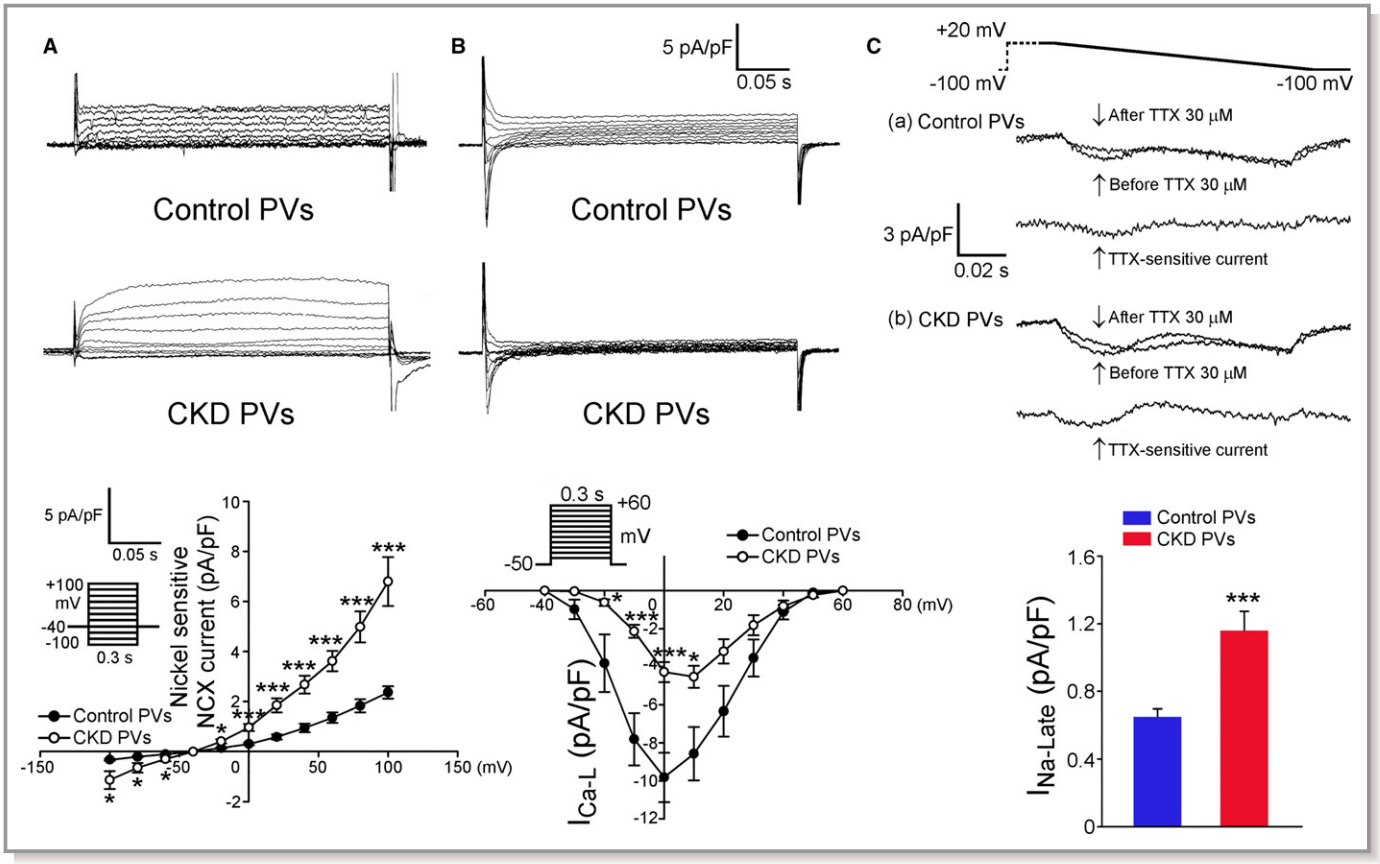

Figure 5. Ionic currents in control and chronic kidney disease (CKD) pulmonary vein (PV) cardiomyocytes. A, Tracings and current-voltage relationship of the sodium/calcium exchanger (NCX) from control (n=9, from 4 hearts) and CKD PV cardiomyocytes (n=10, from 5 hearts). B, Tracings and I–V relationship of L-type calcium currents ($I_{Ca\text{-}L}$) from control (n=10, from 5 hearts) and CKD PV cardiomyocytes (n=10, from 5 hearts). C, Tracings and average data of late sodium currents ($I_{Na\text{-}Late}$) from control (n=11, from 6 hearts) and CKD PV cardiomyocytes (n=13, from 5 hearts). TTX indicates tetrodotoxin. *P<0.05, ***P<0.005 vs control.

higher plasma level of malondialdehyde (10.55±1.14 versus 6.19±1.17 μmol/L) than did control rabbits (n=6). In addition, CKD PV cardiomyocytes (n=6, from 4 hearts) had higher malondialdehyde (40.58±7.34 versus 22.67±3.19 pmol/mg) than did control PV cardiomyocytes (n=6, from 4 hearts). As shown in Figure 8A, MPG (100 μmol/L) reduced calcium transients in CKD PV cardiomyocytes to an extent (1.48±0.08 versus 2.21±0.05 F/F_0) similar to those in H89-treated (1 μmol/L) and control PV cardiomyocytes (Figure 3), which were smaller than those in KN93-treated (1 μmol/L) CKD PV cardiomyocytes. Furthermore, as shown in Figure 8B, we treated MPG in H89- or KN93-treated CKD PV cardiomyocytes and found that MPG decreased calcium transient in KN93-treated (1 μmol/L) CKD PV cardiomyocytes (2.01±0.15 versus 1.62±0.10 F/F_0) but not in H89-treated (1 μmol/L) PV cardiomyocytes (1.59±0.09 versus 1.50±0.10 F/F_0).

Discussion

Our previous study showed that PVs in rabbits with advanced renal failure had rapid and irregular electrical activities due to abnormal calcium regulation and high expression of the NCX protein, which were suppressed by a selective blocker of the outward NCX.[16] CKD is the important risk factor for AF. The excessive APCs, supraventricular tachyarrhythmia, and high PV arrhythmogenesis found in CKD rabbits may increase the risk of AF.[29,30] This study found that CKD PV cardiomyocytes had calcium overload, which may lead to a faster PV beating rate. In addition, CKD PV cardiomyocytes revealed a high frequency of calcium sparks. Increased calcium stores and calcium transient could result in enhanced calcium sparks due to calcium overload or RyR dysfunction in PV cardiomyocytes.[24,31] A more frequent spontaneous SR calcium release was proven to induce great calcium sparks and extensive calcium waves in cardiomyocytes from patients with AF.[5] Moreover, CKD PV cardiomyocytes had a higher frequency, longer duration, width, and peak time of calcium sparks, which were related to enhanced pacemaker activity, than did the controls in our study.[8,31] In addition, the longer decay time of calcium sparks, which was associated with maladaptation of the RyR, may prolong SR calcium release events leading to arrhythmogenesis in CKD PV cardiomyocytes.[32]

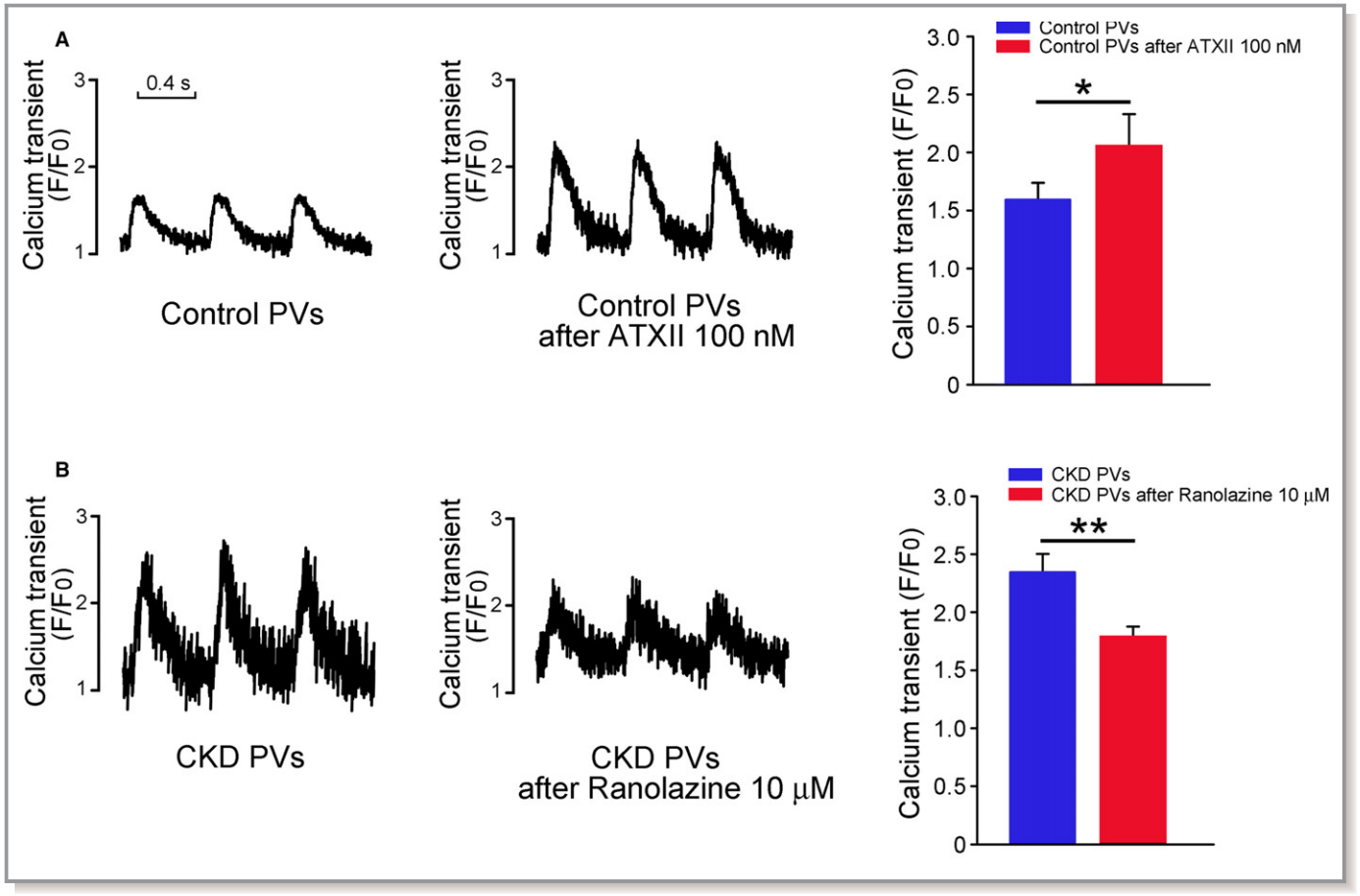

Figure 6. Role of late sodium currents ($I_{Na\text{-}Late}$) in calcium transient in pulmonary vein (PV) cardiomyocytes. A, Tracings and average data of calcium transients from 2-Hz field stimulation in control PV cardiomyocytes (n=10, from 3 hearts) before and after *Anemonia sulcata* toxin (ATXII, 100 nmol/L). B, Tracings and average data of calcium transients from 2-Hz field stimulation in chronic kidney disease (CKD) PV cardiomyocytes (n=10, from 3 hearts) before and after ranolazine (10 μmol/L). *P<0.05, **P<0.01.

In this study, we found that CKD PV cardiomyocytes had higher SERCA2a activity, which increased SR content and led to a higher incidence of calcium spark. Similar to our previous study, the western blot showed that CKD PVs had larger PLB pSer16, which may contribute to their higher SERCA2a activity and calcium overload.[16] Elevated PKA activity in our CKD PV cardiomyocytes can cause RyR dysfunction and raise SERCA2a activity as a result of RyR and PLB phosphorylation.[33] Through single-cell experiments, we found that an inhibitor of PKA eliminated calcium overload and increased calcium sparks in CKD PV cardiomyocytes. These findings highlight the importance of RyR dysfunction or calcium overload along with underlying PKA hyperphosphorylation in the arrhythmogenesis of CKD PV cardiomyocytes. Taken together, CKD PV cardiomyocytes with enhanced kinase activity may lead to calcium overload or calcium transients, which induce the risk of AF.[34] CaMKII was shown to contribute to calcium dysregulation in AF patients.[35] In CKD PV cardiomyocytes, inhibition of CaMKII by KN93 also reduced calcium transients and the incidence of calcium sparks; however, inhibiting CaMKII did not completely eliminate calcium dysregulation in CKD PV cardiomyocytes. These results suggest that activation of PKA rather than CaMKII signaling causes increased PV arrhythmogenesis in CKD. The NCX plays an important role in the genesis of PV electrical activity and calcium homeostasis.[24,36] Our study found an increased NCX current with a larger sodium influx through the $I_{Na\text{-}Late}$ in CKD PV cardiomyocytes. The increase of calcium transient by $I_{Na\text{-}Late}$ enhancer (*Anemonia sulcata* toxin) in control PV cardiomyocytes and the decrease of calcium transient by ranolazine in CKD PV cardiomyocytes suggests that $I_{Na\text{-}Late}$ can induce calcium overload and contribute to the faster PV spontaneous activity.[37]

CKD significantly increases the risk of cardiovascular disease.[38] Previous study has shown that accumulation of uremic toxins in CKD increases oxidative stress, leading to cardiovascular diseases.[39] Increased oxidative stress by uremic toxin of indoxyl sulfate was shown to enhance PV arrhythmogenesis.[40] In addition, oxidative stress potentially contributes to endothelial dysfunction and cardiac hypertrophy in CKD patients.[41,42] The loss of renal energy metabolism,

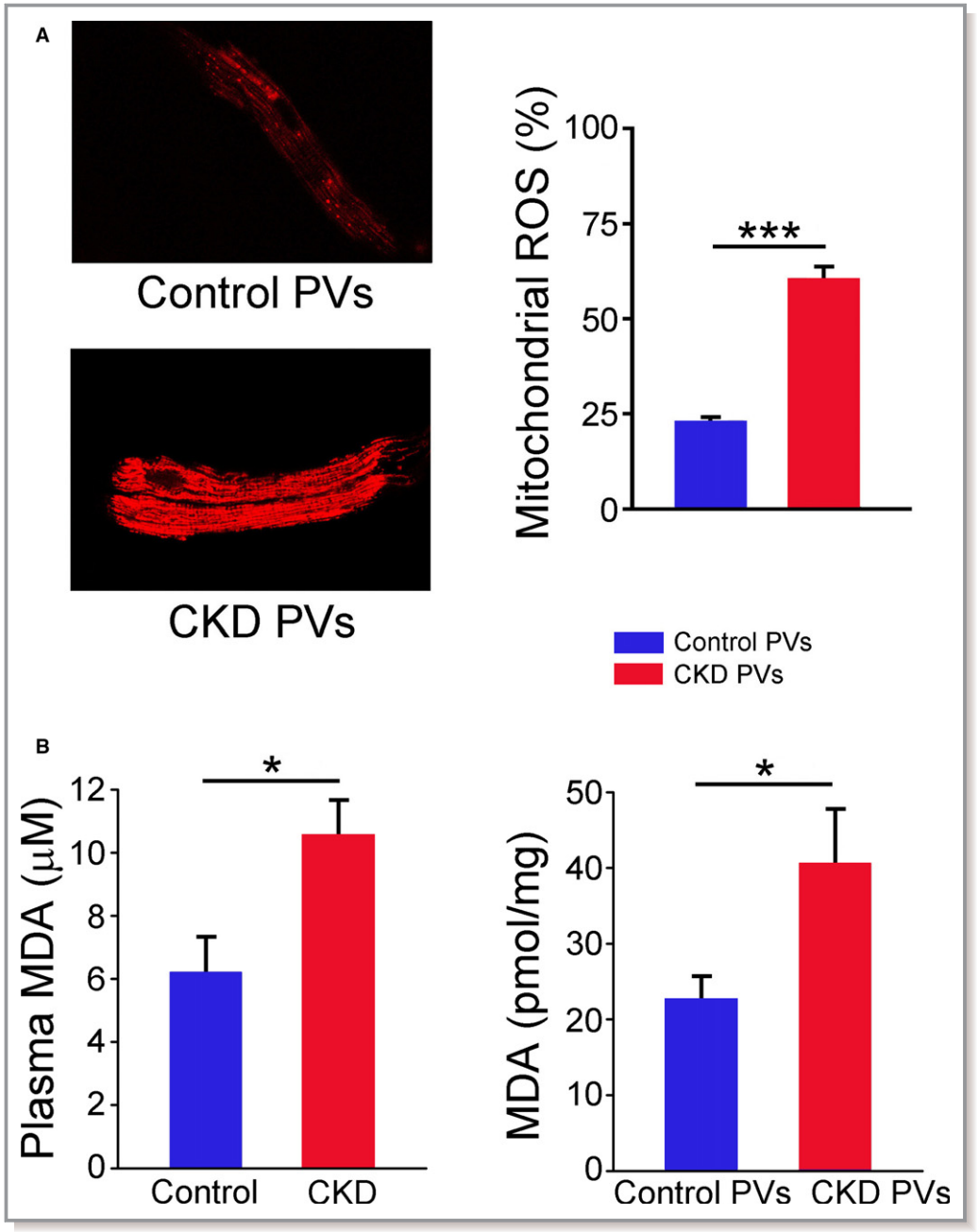

Figure 7. Reactive oxygen species (ROS) in control and chronic kidney disease (CKD) pulmonary vein (PV) cardiomyocytes. A, An example and average data of mitochondrial ROS in control (n=10, from 3 hearts) and CKD (n=8, from 3 hearts) PV cardiomyocytes. B, Average data of plasma and cytosol malondialdehyde (MDA) in control and CKD rabbits and PV cardiomyocytes. **P*<0.05, ****P*<0.005 vs control.

resulting in dyslipidemia and oxidative stress, may increase cardiovascular burden in CKD.[43] Accordingly, increased oxidative stress in CKD is critically associated with cardiovascular diseases. The overproduction of oxidative stress in AF pathogenesis was demonstrated in a human study and in cardiomyocytes of nephrectomy-induced CKD animals.[15,44] In addition, ROS-induced ROS release from mitochondria could contribute to the development of cardiac arrhythmia through abnormal mitochondrial depolarization.[45] This study found that CKD rabbits had increased malondialdehyde in the plasma, and CKD PV cells had enhanced cytosolic malondialdehyde and mitochondrial-specific ROS.[44] Moreover, similar to a PKA inhibitor but not a CaMKII blocker, a ROS scavenger suppressed calcium-handling dysregulation in CKD PV cardiomyocytes. Moreover, this study compared the effects of a ROS scavenger in CaMKII- or PKA-inhibitor–treated CKD PV cardiomyocytes. PKA blockade reduced the inhibitory effects of MPG on calcium transient, suggesting that ROS signaling

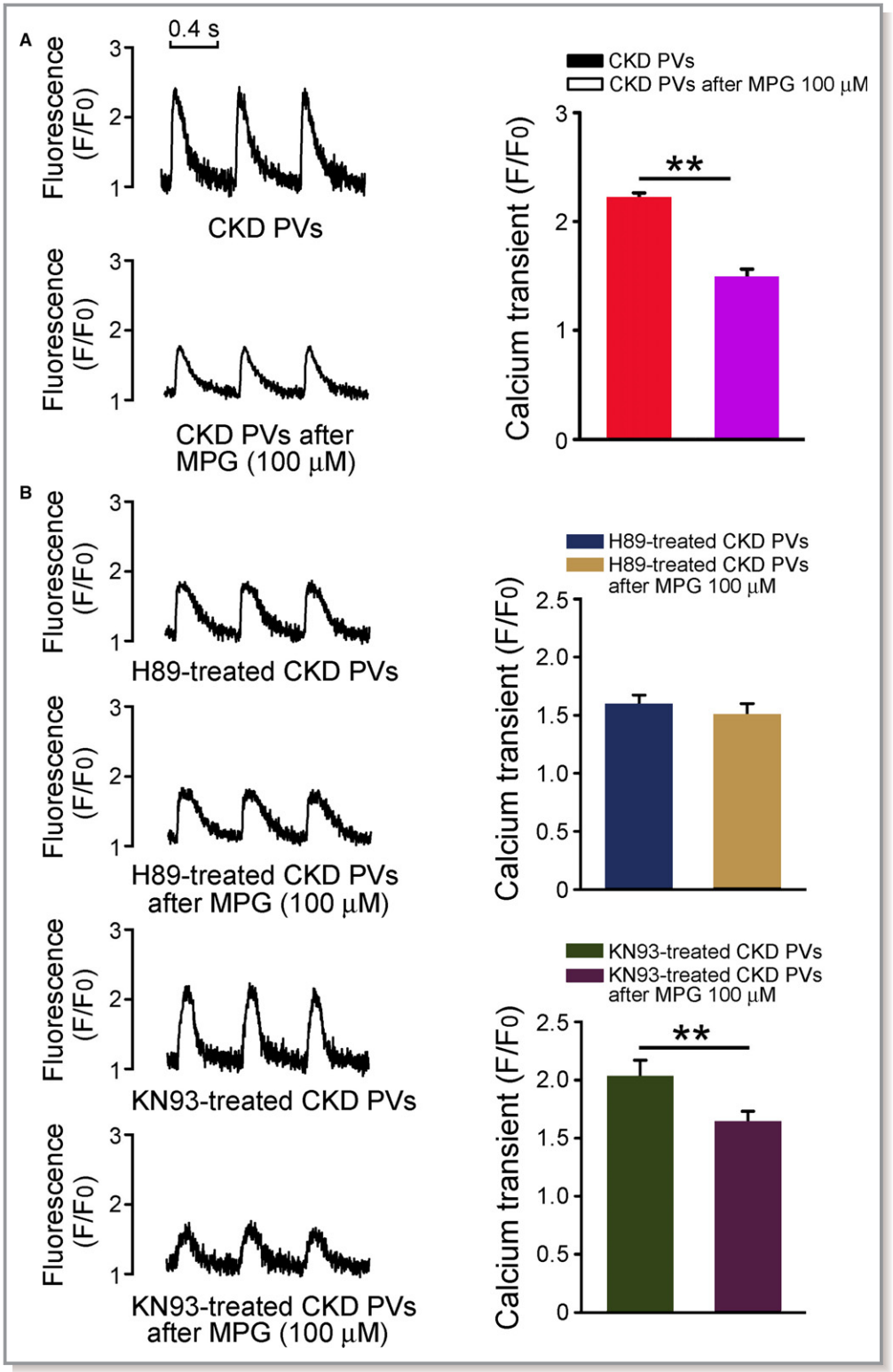

Figure 8. The role of reactive oxygen species (ROS) in control and chronic kidney disease (CKD) pulmonary vein (PV) cardiomyocytes. A, Tracings and average data of calcium transients from 2-Hz field stimulation in CKD PV cardiomyocytes before and after MPG (N-[2-mercaptopropionyl]glycine; 100 μmol/L, n=13, from 4 hearts). MPG-treated CKD PV cardiomyocytes had smaller calcium transients than did CKD PV cardiomyocytes. B, Tracings and average data of calcium transients from 2-Hz field stimulation in CKD PV cardiomyocytes treated with H89 (n=12, from 3 hearts) or KN93 (n=14, from 3 hearts) before and after MPG (100 μmol/L). $^{**}P<0.01$.

through PKA activation may contribute to the high arrhythmogenesis in CKD PV cardiomyocytes.[18,33]

Limitations

In this study, antibiotics-induced CKD exhibited anemia, proteinuria, dyslipidemia, and electrolyte disturbance, which are typical presentations of human CKD[16]; however, CKD may have different etiologies. It is not clear whether our findings can be applied to other CKD models. Although renal dysfunction for 1 month is expected to be chronic when considering the shorter lifespan of rabbits, a longer duration CKD model may have different expressions of oxidative stress or densities of ionic currents in PV arrhythmogenesis. Moreover, we did not detect AF in CKD rabbits, which may be related to the rather short recording time of ECG in the studied animals. Finally, the overproduction of oxidative stress or enhanced PKA signaling in CKD PV cardiomyocytes could be a specific source that triggers downstream signal pathways in CKD related to atrial arrhythmia. Nonetheless, possible interactions of redox and kinase activities were not fully elucidated in our study. Future research is mandatory to clarify the detailed mechanisms.

Conclusions

CKD PV cardiomyocytes enhanced spontaneous activities by calcium overload and calcium leakage. Redox modification could play an important role in the PKA-related calcium dysregulation of CKD PV cardiomyocytes.

Sources of Funding

This study was supported by grants from the Ministry of Science and Technology (MOST104-2314-B-038-071-MY3, MOST105-2314-B-016-035-MY3, MOST105-2628-B-038-012-MY3, MOST105-2314-B-038-026, MOST105-2314-B-038-059-MY3, and MOST105-2314-B-281-004-MY2), Taipei Medical University-Wan Fang Hospital (103TMU-SHH-23, 104swf02, 104swf07, 104-wf-eva-01, 104-wf-eva-03, 104CGH-TMU-03, 105-wf-eva-06, and 105-wf-eva-08), National Defense Medical Center (MAB-106-067), Chi-Mei Medical Center (105CM-TMU-13 and CMNDMC10508), and the Taiwan Heart Rhythm Society (THRS-1501).

Disclosures

None.

References

1. Benjamin EJ, Wolf PA, D'Agostino RB, Silbershatz H, Kannel WB, Levy D. Impact of atrial fibrillation on the risk of death: the Framingham Heart Study. *Circulation*. 1998;98:946–952.
2. Krahn AD, Manfreda J, Tate RB, Mathewson FA, Cuddy TE. The natural history of atrial fibrillation: incidence, risk factors, and prognosis in the Manitoba Follow-Up Study. *Am J Med*. 1995;98:476–484.
3. Chen SA, Hsieh MH, Tai CT, Tsai CF, Prakash VS, Yu WC, Hsu TL, Ding YA, Chang MS. Initiation of atrial fibrillation by ectopic beats originating from the pulmonary veins: electrophysiological characteristics, pharmacological responses, and effects of radiofrequency ablation. *Circulation*. 1999;100:1879–1886.
4. Nattel S. New ideas about atrial fibrillation 50 years on. *Nature*. 2002;415:219–226.
5. Hove-Madsen L, Llach A, Bayes-Genis A, Roura S, Rodriguez Font E, Aris A, Cinca J. Atrial fibrillation is associated with increased spontaneous calcium release from the sarcoplasmic reticulum in human atrial myocytes. *Circulation*. 2004;110:1358–1363.
6. Wongcharoen W, Chen YC, Chen YJ, Chen SY, Yeh HI, Lin CI, Chen SA. Aging increases pulmonary veins arrhythmogenesis and susceptibility to calcium regulation agents. *Heart Rhythm*. 2007;4:1338–1349.
7. Voigt N, Li N, Wang Q, Wang W, Trafford AW, Abu-Taha I, Sun Q, Wieland T, Ravens U, Nattel S, Wehrens XH, Dobrev D. Enhanced sarcoplasmic reticulum Ca^{2+} leak and increased Na^{+}-Ca^{2+} exchanger function underlie delayed afterdepolarizations in patients with chronic atrial fibrillation. *Circulation*. 2012;125:2059–2070.
8. Chang SH, Chen YC, Chiang SJ, Higa S, Cheng CC, Chen YJ, Chen SA. Increased Ca(2+) sparks and sarcoplasmic reticulum Ca(2+) stores potentially determine the spontaneous activity of pulmonary vein cardiomyocytes. *Life Sci*. 2008;83:284–292.
9. Vest JA, Wehrens XH, Reiken SR, Lehnart SE, Dobrev D, Chandra P, Danilo P, Ravens U, Rosen MR, Marks AR. Defective cardiac ryanodine receptor regulation during atrial fibrillation. *Circulation*. 2005;111:2025–2032.
10. Soliman EZ, Prineas RJ, Go AS, Xie D, Lash JP, Rahman M, Ojo A, Teal VL, Jensvold NG, Robinson NL, Dries DL, Bazzano L, Mohler ER, Wright JT, Feldman HI; Chronic Renal Insufficiency Cohort Study G. Chronic kidney disease and prevalent atrial fibrillation: the Chronic Renal Insufficiency Cohort (CRIC). *Am Heart J*. 2010;159:1102–1107.
11. Kannel WB, Wolf PA, Benjamin EJ, Levy D. Prevalence, incidence, prognosis, and predisposing conditions for atrial fibrillation: population-based estimates. *Am J Cardiol*. 1998;82:2N–9N.
12. Horio T, Iwashima Y, Kamide K, Tokudome T, Yoshihara F, Nakamura S, Kawano Y. Chronic kidney disease as an independent risk factor for new-onset atrial fibrillation in hypertensive patients. *J Hypertens*. 2010;28:1738–1744.
13. Ananthapanyasut W, Napan S, Rudolph EH, Harindhanavudhi T, Ayash H, Guglielmi KE, Lerma EV. Prevalence of atrial fibrillation and its predictors in nondialysis patients with chronic kidney disease. *Clin J Am Soc Nephrol*. 2010;5:173–181.
14. Ehrlich JR, Hohnloser SH, Nattel S. Role of angiotensin system and effects of its inhibition in atrial fibrillation: clinical and experimental evidence. *Eur Heart J*. 2006;27:512–518.
15. Fukunaga N, Takahashi N, Hagiwara S, Kume O, Fukui A, Teshima Y, Shinohara T, Nawata T, Hara M, Noguchi T, Saikawa T. Establishment of a model of atrial fibrillation associated with chronic kidney disease in rats and the role of oxidative stress. *Heart Rhythm*. 2012;9:2023–2031.
16. Huang SY, Chen YC, Kao YH, Hsieh MH, Chen YA, Chen WP, Lin YK, Chen SA, Chen YJ. Renal failure induces atrial arrhythmogenesis from discrepant electrophysiological remodeling and calcium regulation in pulmonary veins, sinoatrial node, and atria. *Int J Cardiol*. 2016;202:846–857.
17. Xu Y, Osborne BW, Stanton RC. Diabetes causes inhibition of glucose-6-phosphate dehydrogenase via activation of PKA, which contributes to oxidative stress in rat kidney cortex. *Am J Physiol Renal Physiol*. 2005;289:F1040–F1047.
18. Wagner S, Rokita AG, Anderson ME, Maier LS. Redox regulation of sodium and calcium handling. *Antioxid Redox Signal*. 2013;18:1063–1077.
19. Viatchenko-Karpinski S, Kornyeyev D, El-Bizri N, Budas G, Fan P, Jiang Z, Yang J, Anderson ME, Shryock JC, Chang CP, Belardinelli L, Yao L. Intracellular Na^{+} overload causes oxidation of CaMKII and leads to Ca^{2+} mishandling in isolated ventricular myocytes. *J Mol Cell Cardiol*. 2014;76:247–256.
20. Liu T, O'Rourke B. Enhancing mitochondrial Ca^{2+} uptake in myocytes from failing hearts restores energy supply and demand matching. *Circ Res*. 2008;103:279–288.
21. Iwamoto T, Pan Y, Wakabayashi S, Imagawa T, Yamanaka HI, Shigekawa M. Phosphorylation-dependent regulation of cardiac Na^{+}/Ca^{2+} exchanger via protein kinase C. *J Biol Chem*. 1996;271:13609–13615.
22. Goldhaber JI. Free radicals enhance Na^{+}/Ca^{2+} exchange in ventricular myocytes. *Am J Physiol*. 1996;271:H823–H833.

23. Kim SH, Jang YW, Hwang P, Kim HJ, Han GY, Kim CW. The renoprotective effect of a phosphoinositide 3-kinase inhibitor wortmannin on streptozotocin-induced proteinuric renal disease rats. *Exp Mol Med*. 2012;44:45–51.
24. Lkhagva B, Chang SL, Chen YC, Kao YH, Lin YK, Chiu CT, Chen SA, Chen YJ. Histone deacetylase inhibition reduces pulmonary vein arrhythmogenesis through calcium regulation. *Int J Cardiol*. 2014;177:982–989.
25. Huang S-Y, Lu Y-Y, Chen Y-C, Chen W-T, Lin Y-K, Chen S-A, Chen Y-J. Hydrogen peroxide modulates electrophysiological characteristics of left atrial myocytes. *Acta Cardiol Sin*. 2014;30:38–45.
26. Lu Y, Yue L, Wang Z, Nattel S. Effects of the diuretic agent indapamide on Na^+, transient outward, and delayed rectifier currents in canine atrial myocytes. *Circ Res*. 1998;83:158–166.
27. Chu A, Fill M, Stefani E, Entman ML. Cytoplasmic Ca^{2+} does not inhibit the cardiac muscle sarcoplasmic reticulum ryanodine receptor Ca^{2+} channel, although Ca(2+)-induced Ca^{2+} inactivation of Ca^{2+} release is observed in native vesicles. *J Membr Biol*. 1993;135:49–59.
28. Münch G, Bolck B, Karczewski P, Schwinger RH. Evidence for calcineurin-mediated regulation of SERCA 2a activity in human myocardium. *J Mol Cell Cardiol*. 2002;34:321–334.
29. Binici Z, Intzilakis T, Nielsen OW, Kober L, Sajadieh A. Excessive supraventricular ectopic activity and increased risk of atrial fibrillation and stroke. *Circulation*. 2010;121:1904–1911.
30. Ozcan C, Strom JB, Newell JB, Mansour MC, Ruskin JN. Incidence and predictors of atrial fibrillation and its impact on long-term survival in patients with supraventricular arrhythmias. *Europace*. 2014;16:1508–1514.
31. Chang SL, Chen YC, Yeh YH, Lin YK, Wu TJ, Lin CI, Chen SA, Chen YJ. Heart failure enhanced pulmonary vein arrhythmogenesis and dysregulated sodium and calcium homeostasis with increased calcium sparks. *J Cardiovasc Electrophysiol*. 2011;22:1378–1386.
32. Zima AV, Picht E, Bers DM, Blatter LA. Termination of cardiac Ca^{2+} sparks: role of intra-SR $[Ca^{2+}]$, release flux, and intra-SR Ca^{2+} diffusion. *Circ Res*. 2008;103:e105–e115.
33. Kohler AC, Sag CM, Maier LS. Reactive oxygen species and excitation-contraction coupling in the context of cardiac pathology. *J Mol Cell Cardiol*. 2014;73:92–102.
34. Chen YJ, Chen YC, Wongcharoen W, Lin CI, Chen SA. Effect of K201, a novel antiarrhythmic drug on calcium handling and arrhythmogenic activity of pulmonary vein cardiomyocytes. *Br J Pharmacol*. 2008;153:915–925.
35. Xie LH, Chen F, Karagueuzian HS, Weiss JN. Oxidative-stress-induced afterdepolarizations and calmodulin kinase II signaling. *Circ Res*. 2009;104:79–86.
36. Chang CJ, Cheng CC, Yang TF, Chen YC, Lin YK, Chen SA, Chen YJ. Selective and non-selective non-steroidal anti-inflammatory drugs differentially regulate pulmonary vein and atrial arrhythmogenesis. *Int J Cardiol*. 2015;184:559–567.
37. Huang SY, Chen YC, Kao YH, Hsieh MH, Lin YK, Chung CC, Lee TI, Tsai WC, Chen SA, Chen YJ. Fibroblast growth factor 23 dysregulates late sodium current and calcium homeostasis with enhanced arrhythmogenesis in pulmonary vein cardiomyocytes. *Oncotarget*. 2016;7:69231–69242.
38. Sarnak MJ, Levey AS, Schoolwerth AC, Coresh J, Culleton B, Hamm LL, McCullough PA, Kasiske BL, Kelepouris E, Klag MJ, Parfrey P, Pfeffer M, Raij L, Spinosa DJ, Wilson PW; American Heart Association Councils on Kidney in Cardiovascular Disease HBPRCC, Epidemiology, Prevention. Kidney disease as a risk factor for development of cardiovascular disease: a statement from the American Heart Association Councils on Kidney in Cardiovascular Disease, High Blood Pressure Research, Clinical Cardiology, and Epidemiology and Prevention. *Hypertension*. 2003;42:1050–1065.
39. Moradi H, Sica DA, Kalantar-Zadeh K. Cardiovascular burden associated with uremic toxins in patients with chronic kidney disease. *Am J Nephrol*. 2013;38:136–148.
40. Chen WT, Chen YC, Hsieh MH, Huang SY, Kao YH, Chen YA, Lin YK, Chen SA, Chen YJ. The uremic toxin indoxyl sulfate increases pulmonary vein and atrial arrhythmogenesis. *J Cardiovasc Electrophysiol*. 2015;26:203–210.
41. Cachofeiro V, Goicochea M, de Vinuesa SG, Oubina P, Lahera V, Luno J. Oxidative stress and inflammation, a link between chronic kidney disease and cardiovascular disease. *Kidney Int Suppl*. 2008;111:S4–S9.
42. Martinez-Vea A, Marcas L, Bardaji A, Romeu M, Gutierrez C, Garcia C, Compte T, Nogues R, Peralta C, Giralt M. Role of oxidative stress in cardiovascular effects of anemia treatment with erythropoietin in predialysis patients with chronic kidney disease. *Clin Nephrol*. 2012;77:171–181.
43. Vaziri ND. Role of dyslipidemia in impairment of energy metabolism, oxidative stress, inflammation and cardiovascular disease in chronic kidney disease. *Clin Exp Nephrol*. 2014;18:265–268.
44. Leftheriotis DI, Fountoulaki KT, Flevari PG, Parissis JT, Panou FK, Andreadou IT, Venetsanou KS, Iliodromitis EK, Kremastinos DT. The predictive value of inflammatory and oxidative markers following the successful cardioversion of persistent lone atrial fibrillation. *Int J Cardiol*. 2009;135:361–369.
45. Akar FG, Aon MA, Tomaselli GF, O'Rourke B. The mitochondrial origin of postischemic arrhythmias. *J Clin Invest*. 2005;115:3527–3535.